Seventh Canadian Masonry Symposium
McMaster University
Hamilton, Ontario
June 4-7, 1995

RESPONSE OF REINFORCED CONCRETE MASONRY SHEAR WALLS

K. S. Ibrahim[1] and G.T. Suter[2]

ABSTRACT

Analytical and experimentally based models are needed to predict the behaviour of reinforced masonry buildings under different complex states of stress and to assess the behavioural seismic characteristics of masonry buildings undergoing progressive failure up to the ultimate stage. As part of an experimental and theoretical study addressing the aforementioned needs, five reinforced concrete masonry shear walls were tested under a cyclic shear load pattern to examine the influence of the applied axial stress, the amount of vertical reinforcement and the wall aspect ratio on the lateral resistance and failure mechanism. The load/displacement relationship was traced up to the maximum lateral resistance and beyond to study the softening behaviour of the cracked reinforced masonry systems undergoing brittle shear-dominated progressive failures.

In this paper, the experimental study is summarized and results are compared with numerical values obtained from nonlinear finite element analyses. Good correlation between the numerical and experimental results was obtained.

[1]Doctoral candidate, Department of Civil and Environmental Engineering, Carleton University, Ottawa, Ontario, K1S 5B6.

[2]Professor, Department of Civil Engineering and Environmental Engineering, Carleton University, Ottawa, Ontario, K1S 5B6.

INTRODUCTION

Lateral motion will result when buildings are subjected to lateral ground shaking due to passage of seismic waves. This motion will induce additional forces and stresses on the lateral load-resisting structural elements. In multi-storey masonry buildings, reinforced masonry shear walls usually form the lateral seismic load resistance elements. The design of reinforced masonry shear walls for all critical seismic limit states requires a detailed understanding of the complete reversed cyclic response. Therefore, large scale experimental data are necessary to establish behavioural characteristics of masonry shear walls subjected to cyclic loading before comprehensive and representative design models can be developed.

SCOPE AND OBJECTIVES

To investigate the complete nonlinear response of structural components under seismic loading, increasing cyclic quasi-static experiments are frequently performed. Data from full-scale experimental studies on masonry shear walls are necessary to establish behavioural characteristics of masonry assemblages under cyclic loading at cracking, yielding, crushing, peak strength and deformation limit states before comprehensive and representative design models can be developed.

To develop a model for predicting the shear strength of a reinforced masonry wall exhibiting shear brittle failure, certain mechanisms need to be modeled and the extension of the effect of certain parameters need to be investigated. In the current experimental investigation, the effects of aspect ratio, applied axial stress and amount of vertical reinforcement on the residual lateral strength of reinforced masonry shear walls were investigated experimentally.

TEST SPECIMENS

A total of five 1400 mm high reinforced masonry walls were subjected to lateral cyclic reversed displacement patterns simulating earthquake excitation while a constant precompressive vertical load was applied to simulate the dead load of the structure. Each wall was built of 140 $\times$ 190 $\times$ 400 mm hollow concrete blocks in single wythe construction. Details of the test walls including geometry, reinforcement ratios and loading conditions are given in Table 1.

All the walls were designed to experience brittle shear failure modes accompanied by diagonal cracking. The first three specimens had aspect ratios (height/length) of 1.0, 0.636 and 0.467 respectively. These three wall panels had the same vertical and horizontal reinforcement percentages of 0.4 % and 0.2 % respectively, and were tested under a constant applied vertical compressive stress of 0.69 MPa (100 psi) as shown in Table 1. Test results of these three specimens (designated walls 1, 2 and 3) were used to determine the effect of aspect ratio on the shear strength of reinforced masonry

shear walls.

In studying the effect of the amount of vertical reinforcement on the lateral shear resistance of reinforced masonry panels, a reinforced masonry wall panel, designated wall 4, with an aspect ratio of 0.636 was tested under a vertical stress of 0.69 MPa (100 psi). The wall had vertical and horizontal reinforcement ratios of 0.6% and 0.2%, respectively.

Also, to investigate the effect of the applied compressive stress on the lateral resistance of masonry panels, a reinforced masonry wall panel, designated wall 5, with an aspect ratio of 0.636 was tested under a vertical stress of 1.73 MPa (250 psi). The wall had vertical and horizontal reinforcement ratios of 0.4 % and 0.2%, respectively.

The reinforcement ratios were chosen to ensure a shear dominated failure mode. All walls were modeled using a newly developed nonlinear finite element model to predict their modes of failure. All walls were fully grouted with vertical and horizontal reinforcement spaced uniformly at 400 mm. The horizontal reinforcing bars were placed at the middle height of a course by knocking off the cross webs to half-height of the block. The horizontal reinforcement had 180° hooks around the extreme vertical steel at both far ends. The vertical reinforcement ran continuously from the base block to the top block and was properly anchored. All reinforcing bars were of Grade 400.

TEST SETUP

The test setup is shown in Fig. 1. A displacement controlled 667 kN (150 kips) hydraulic actuator was used to apply lateral loads to the shear walls. Vertical loads were applied by means of four Dywidag bars anchored underneath the strong floor and stressed against the top concrete block of each specimen through stiff coil springs. The vertical pressure was applied using an electric pump connected to hydraulic jacks mounted over the top of the concrete block. For walls no. 1, 2, 4 and 5, two 10-ton jacks were used at the top of each wall while, for wall no. 3 (the longest wall), four 10-ton jacks were employed to ensure a uniformly distributed vertical stress. The electric pump with a self-adjusted hydraulic pressure system provided a constant vertical pressure during testing.

INSTRUMENTATION

Readings of the applied vertical and horizontal loads as well as deformations at the key points of the specimens were recorded. Linear Variable Differential Transducers (LVDT's) were used to monitor the lateral deflection, flexural deformation, shear deformation, base slip, and base uplift of each specimen. Seventeen LVDT's were used to monitor the wall's deformational behaviour as shown in Fig. 2.

Electrical resistance strain gauges were placed on the vertical reinforcement within the

most highly stressed region at the joint between the wall and the footing to monitor the first yield as well as the distribution of the tensile strain in the vertical steel bars.

LOAD/DISPLACEMENT SEQUENCES

Each specimen was subjected to a prescribed lateral displacement history under a constant axial load. A standard lateral displacement history as shown in Fig. 3 was employed. The displacement history consisted of sequences of fully reversed displacement cycles. The displacement amplitude of the first cycle of each sequence was identical to the maximum amplitude of the previous sequence; the first cycle was followed by three cycles of an increased amplitude, and finally by one cycle of decaying amplitude. The decay cycle had an amplitude of one-half of the maximum amplitude of the sequence. The sequence was repeated, with an amplitude increment each time, until the specimen lost 50% of its maximum load resistance or the displacement limit of the horizontal actuator was reached.

ANALYTICAL MODEL

For all the analyses presented in this paper, a smeared crack finite element based model was developed (Ibrahim and Suter, 1994) and utilized to simulate the reinforced masonry post-crushing and post-cracking behaviour.

Three finite element meshes to model the wall panels are shown in Fig. 4. The modeled walls were subjected to displacement-controlled sequences by specifying horizontal displacement increments at the top nodes while a constant uniformly distributed axial load was applied at the beginning of the incremental analysis. Both monotonic and cyclic displacement sequences were considered in the numerical analyses. Eight node quadrilaterals with 3 × 3 Gauss points were used in the current analysis.

Masonry Compressive Stress-Strain Relationship

Bathe and Ramaswamy (Bathe and Ramaswamy, 1979) have derived a stress-strain relation for concrete or rock material based on tests for concrete under uniaxial compressive stress. This model was adapted for masonry where the principal compressive stress-strain law of grouted masonry (f_m, ϵ_m) was assumed as

$$f_m = \frac{f'_m(E_o/E_s)(\epsilon_m/\epsilon_o)}{1 + A(\epsilon_m/\epsilon_o) + B(\epsilon_m/\epsilon_o)^2 + C(\epsilon_m/\epsilon_o)^3} \tag{1}$$

where

$A = \frac{[E_o/E_u + (p^3-2p^2)E_o/E_s - (2p^3-3p^2+1)]}{[(p^2-2p+1)p]}$, $\quad B = [(2E_o/E_s - 3) - 2A]$,

and $C = [(2 - E_o/E_s) + A]$

The strength parameters $E_o, f'_m, \epsilon_o, E_s = f'_m/\epsilon_o, f_{um}, \epsilon_{um}, p = \epsilon_{um}/\epsilon_o$ and, $E_u = f_{um}/\epsilon_{um}$ are obtained from uniaxial tests where

ϵ_o = strain at uniaxial peak compressive stress

f_{um}, ϵ_{um} = uniaxial ultimate compressive stress and corresponding strain.

Employing failure envelopes to establish the uniaxial stress-strain law accounting for multiaxial stress conditions, the crushing stress value is calculated as $\tilde{f}'_m$, and a ratio $\gamma_1 = \tilde{f}'_m/f'_m$ can be determined. Therefore, one can find:

$\tilde{f}_{um} = \gamma_1 f_{um}$, $\tilde{\epsilon}_o = \gamma_1\gamma\epsilon_o$, and $\tilde{\epsilon}_{um} = \gamma_1\gamma\epsilon_{um}$

where γ is a constant and $\tilde{f}'_m$, $\tilde{f}_{um}$, $\tilde{\epsilon}_o$, and $\tilde{\epsilon}_{um}$ are employed in order to establish the uniaxial stress-strain law under multiaxial conditions.

Tension-Stiffening Models for Masonry

Similar to concrete, as the masonry reaches its tensile strength, primary cracks form and their number and extent are controlled by the size and placement of the reinforcing steel. At the primary cracks, the masonry stress drops to zero and the steel carries the full load. However, the masonry between cracks still maintains some tensile resistance which will drop as the load increases. The drop will be associated with the breakdown in bond and a secondary system of internal cracks will develop around the reinforcement.

Gopalaratnam and Shah (Gopalaratnam and Shah, 1985) have proposed an analytical model which assumes a unique stress-strain relationship only in the ascending part and a unique relationship only between stress and crack width in the descending part. This was deduced from results obtained from an experimental program carried out on different concrete, mortar, and paste specimens subjected to tensile stress.

For the ascending part, a simple expression that has been employed for defining compressive behaviour of concrete was used (Shah *et al.*, 1983) for the uniaxial tensile stress-strain curve up to the peak stress value:

$$f_m = f_{mcr}[1 - (1 - \frac{\epsilon_m}{\epsilon_{mcr}})^A] \qquad (2)$$

where

f_m = tensile stress, f_{mcr} = peak value of f_m, ϵ_m = tensile strain, ϵ_{mcr} = value of strain, ϵ_m, at f_{mcr}, A = $E_t\epsilon_{mcr}/f_{mcr}$, and E_t = initial tangent modulus.

For the descending part, due to the localized nature of the post-peak deformations, no unique stress-strain relationship existed. Instead, Gopalaratnam and Shah found a unique relationship between average stress and average crack width in the form:

$$f_m = f_{mcr}(e^{-kw^{\lambda}}) \tag{3}$$

where w is the crack width, and k and λ are constants.

Bazant and Oh (Bazant and Oh, 1983) have proposed the *crack band model* where the front of an advancing crack band (microcrack zone), called the fracture process zone, has a certain characteristic width w_c which is a function of the maximum aggregate size. Now a new term, *fracture process zone strain*, ϵ_f, can be defined as the ratio between the sum of individual microcrack openings, δ_f, and the crack band width w_c.

$$\epsilon_f = \frac{\delta_f}{w_c} \tag{4}$$

where

$$w_c = \eta d_a \tag{5}$$

w_c = crack band width
η = constant (between 1.5 and 4)
d_a = maximum aggregate size.

Therefore, based on results by Gopalaratnam and Shah, and on the existing relationship between the post-peak cracking stress and crack width, and also utilizing the *crack band model* of the fracture process zone developed by Bazant and Oh, the total strain of a domain loaded in tension is equal to the sum of three main components as follows:

$$\epsilon_t = \epsilon_e + \epsilon_{mp} + \epsilon_f \tag{6}$$

where

$\epsilon_e = \frac{f_m}{E_t}$
$\epsilon_{mp} = \epsilon_{mcr} - \frac{f_{mcr}}{E_t}$
$\epsilon_f = \frac{1}{w_c}(-\frac{1}{k} ln \frac{f_m}{f_{mcr}})^{\frac{1}{\lambda}}$

and

$$\epsilon_t = \frac{f_m}{E_t} + \epsilon_{mcr} - \frac{f_{mcr}}{E_t} + \frac{1}{w_c}(-\frac{1}{k} ln \frac{f_m}{f_{mcr}})^{\frac{1}{\lambda}} \quad (7)$$

ANALYSIS AND DISCUSSION

For wall 1, Fig. 5 illustrates a comparison between the experimental load-top displacement hysteresis curves and the monotonic analytical prediction using the finite element mesh illustrated in Fig. 4(a). It can be seen that the analytical model envelope closely matches the experimental results. Also, the numerical model exhibited ductile behaviour similar to the test wall. The ultimate load predicted by the numerical model was 214 kN as compared to the test wall's 209 kN in the positive and -200 kN in the negative loading directions, respectively.

For wall 3, Fig. 6 illustrates a comparison between the experimental load-top displacement hysteresis curves and the monotonic analytical prediction using the finite element mesh illustrated in Fig. 4(c). It can be seen that while the analytical model envelope closely matches the experimental results up to 75% of the ultimate load, the load-deflection envelope showed slight discrepancies compared to the experimental results above this limit. Also, the numerical model exhibited brittle behaviour as experienced by the test wall. The ultimate load predicted by the numerical model was 575 kN compared with 553 kN in the positive and -529 kN in the negative loading directions, respectively.

The analysis of the flexure dominated wall 1 indicated a good match with the experimental results. On the other hand, the analyses of the shear dominated wall 3 indicated a slight increase in the wall's lateral resistance over the experimental results and this occurred at slightly smaller displacement values. The analytical model successfully captured the sudden drop in the resistance of the shear walls similar to that experienced experimentally soon after reaching their respective ultimate loads. This sudden drop in strength can be explained as the result of widening of the diagonal crack followed by a substantial reduction in the aggregate-interlock forces and in the residual shear at the crack interface. This reduction is a function of the amount of shear reinforcement (mainly the horizontal steel). This mechanism, to a great extent, was predicted by the newly developed current model. Numerical results, using the current model, indicated no spurious shear strength for the modeled shear dominated walls and the sudden drop due to the excessive opening of the diagonal crack has been properly represented.

CONCLUSIONS

Based on the experimental findings and the analytical study of the behaviour of reinforced masonry shear walls, the following conclusions are reached:

1. For flexure dominated walls, the analytical load-displacement history matches well the experimental envelope curve. The vertical steel yielding pattern due to the widening of flexural cracks and the extent of the crushing is very similar to that observed experimentally. Close prediction for the wall maximum load resistance was found.
2. For shear dominated walls, the analytical load-displacement history matches well the experimental envelope curve. The maximum lateral load resistance predicted by the analytical model is slightly higher than that shown in tests and occurs at a slightly lower lateral displacement value. Numerical results, using the current model, indicated no spurious shear strength for the modeled shear dominated walls and the sudden load decrease due to the excessive opening of the diagonal crack has been properly captured.

ACKNOWLEDGEMENTS

The authors acknowledge with thanks the financial support provided by the Natural Sciences and Engineering Research Council of Canada.

REFERENCES

Bathe, K.J., and Ramaswamy, S., "On Three-Dimensional Nonlinear Analysis of Concrete Structures", Nuclear Engineering and Design, No. 52, 1979, pp. 385-409.

Bazant, Z.P., and Oh, B.H., "Crack Band Theory for Fracture of Concrete", Materials and Structures, Research and Testing (RILEM, Paris), V. 16, No. 93, May-June 1983, pp. 155-177.

Gopalaratnam, V.S., and Shah, S.P., "Softening Response of Plain Concrete in Direct Tension", ACI Journal, May-June 1985, pp. 310-323.

Ibrahim, K.S and Suter, G.T., "Smeared Crack Model for Reinforced Concrete Masonry Shear Wall Analysis", Proceedings, 10th International Brick/Block Masonry Conference, Calgary, July 1994.

Shah, S.P., Fafitis, A., and Arnold, R., "Cyclic Loading of Spirally Reinforced Concrete", Journal of Structural Engineering, ASCE, V. 109, No. 7, July 1983, pp. 1695-1710.

Table 1 Details of masonry wall specimens

Test Wall No.	Wall Aspect Ratio	A_s, vertical	ρ_v (%)	A_s, horizontal	ρ_h (%)	Additional Vertical Stress (MPa)
1	1.000	4# 15 M	0.4	4# 10 M	0.2	0.69 (100 psi)
2	0.636	6# 15 M	0.4	4# 10 M	0.2	0.69 (100 psi)
3	0.467	8# 15 M	0.4	4# 10 M	0.2	0.69 (100 psi)
4	0.636	6# 20 M	0.6	4# 10 M	0.2	0.69 (100 psi)
5	0.636	6# 15 M	0.4	4# 10 M	0.2	1.73 (250 psi)

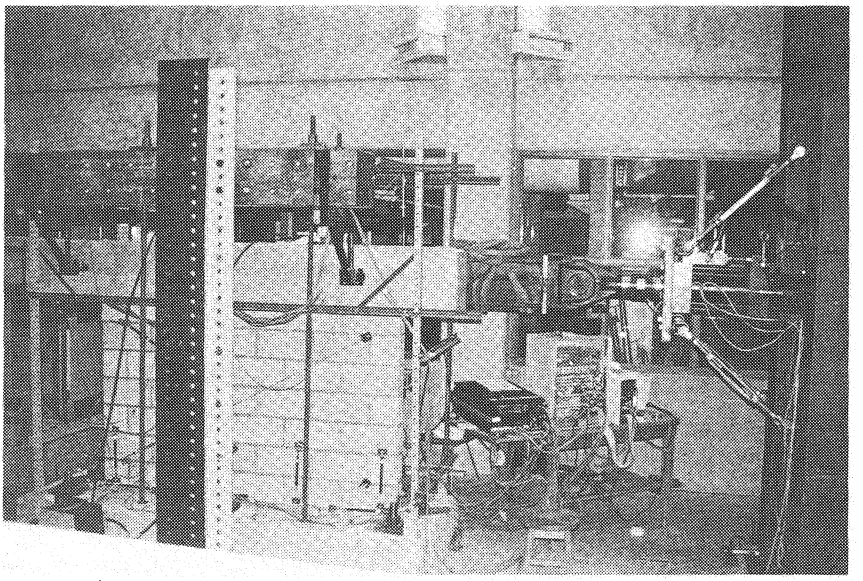

Fig. 1 Test setup.

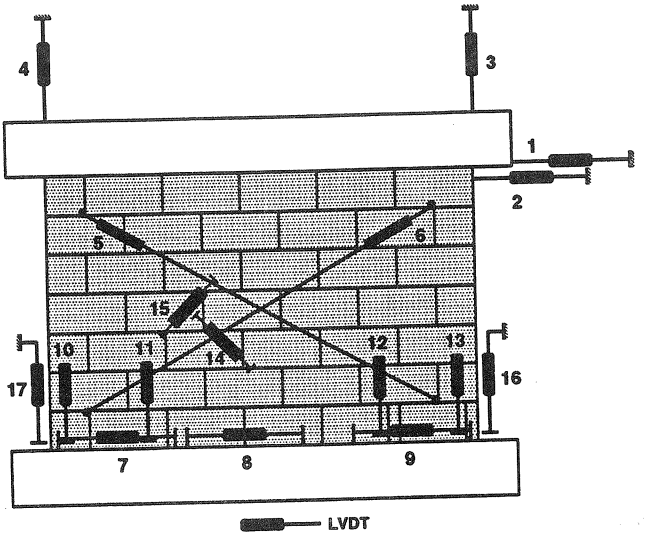

Fig. 2 Arrangement of LVDT's.

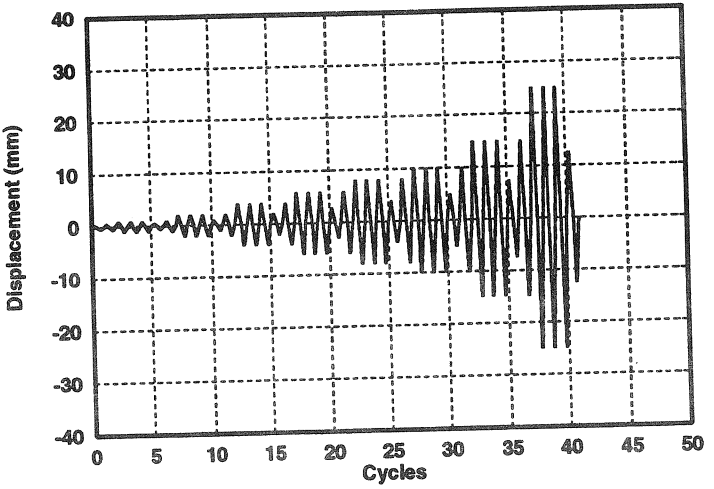

Fig. 3 Displacement history.

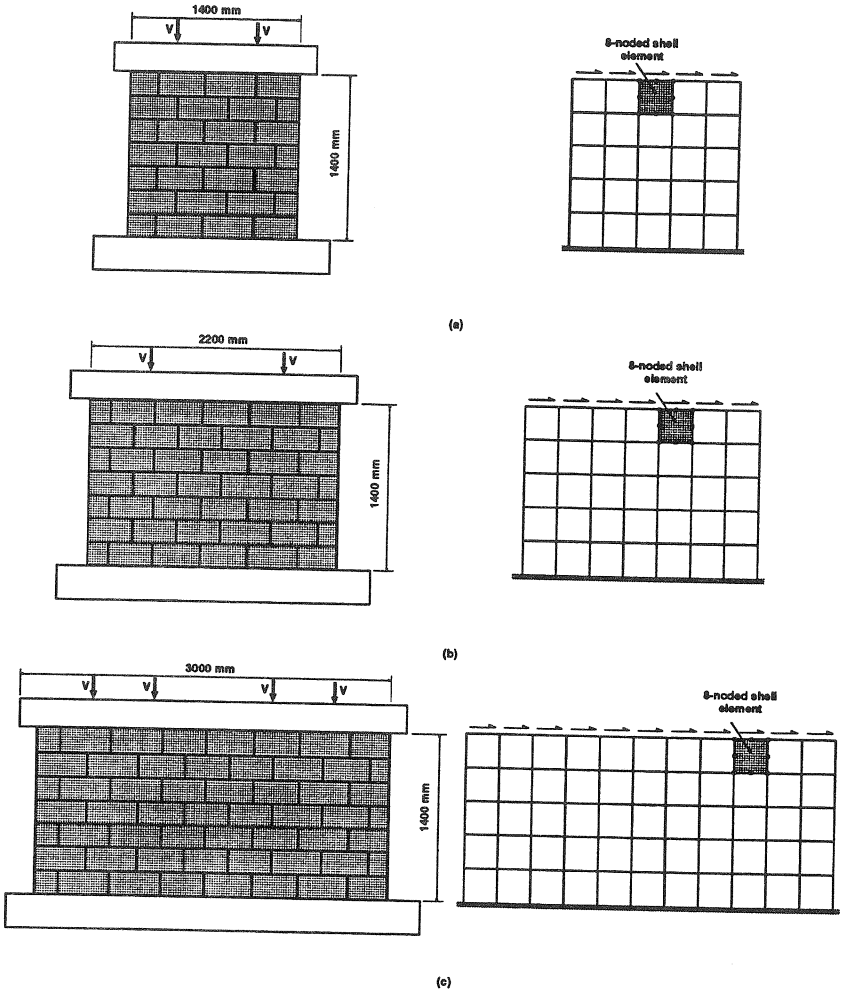

Fig. 4 Test specimens and finite element discretization.

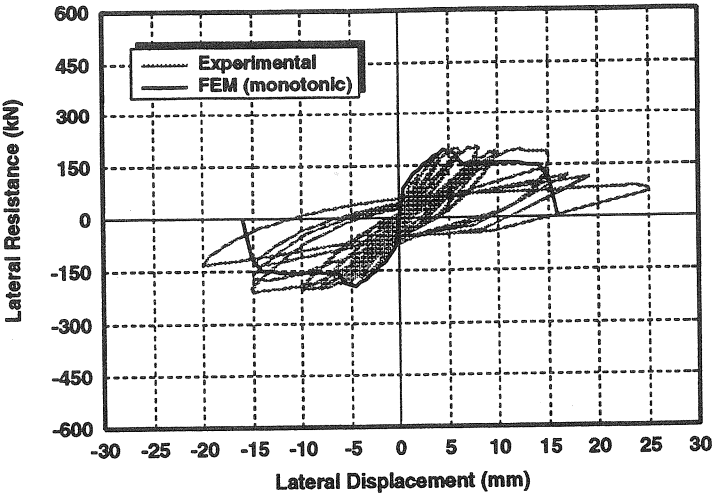

Fig. 5 Comparison of analytical and experimental results for wall 1.

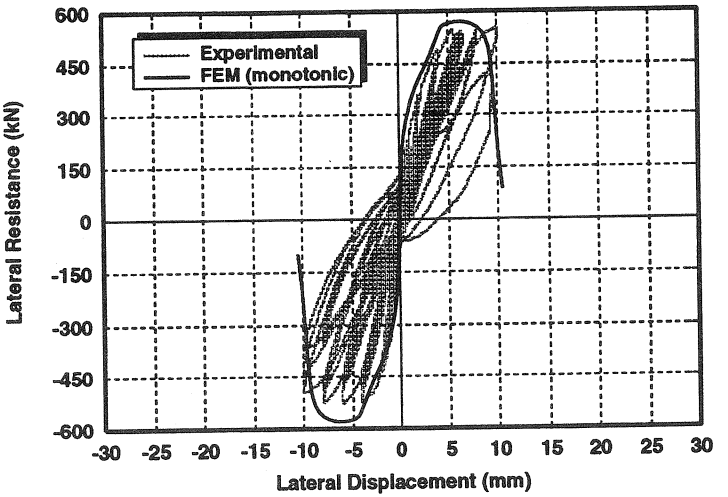

Fig. 6 Comparison of analytical and experimental results for wall 3.